Helmholtz-Zentrum Dresden-Rossendorf (HZDR)

HELMHOLTZ ZENTRUM
DRESDEN ROSSENDORF

Novel Identifier of Transitions in Bubble Columns Operated with Water and Aqueous Alcohol Solutions

Nedeltchev, S. N.; Marchini, S.; Schubert, M.; Hlawitschka, M. W.; Hampel, U.;

Originally published:

July 2023

Chemical Engineering & Technology 46(2023)9, 1782-1790

DOI: https://doi.org/10.1002/ceat.202300095

Perma-Link to Publication Repository of HZDR:

https://www.hzdr.de/publications/Publ-36876

Release of the secondary publication
on the basis of the German Copyright Law § 38 Section 4.

Author 1: Stoyan Nedeltchev[1*]

Author 2: Sara Marchini[2,3]

Author 3: Markus Schubert[4]

Author 4: Mark W. Hlawitschka[5]

Author 5: Uwe Hampel[2,3]

Title of the manuscript:

Novel Identifier of Transitions in Bubble Columns Operated with Water and Aqueous Alcohol Solutions

Abstract

The accurate identification of the transition velocities U_{trans} in bubble columns (BCs) is very important for their effective design, operation and scale-up. In this work, a novel parameter (new hybrid index (NHI)) has been developed and successfully applied to gas holdup and pressure fluctuations recorded in various BCs operated with water and aqueous solutions of alcohols (ethanol and iso-propanol).

The first U_{trans} has been identified on the basis of a well-pronounced local NHI minimum, whereas the second U_{trans} has been distinguished by the point, from which the NHI profile levels off. It has been concluded that the main U_{trans} depend on the type of gas-liquid system and sparger used. A set of several U_{trans} has been reported.

Keywords: Bubble columns, Gas holdup fluctuations, Main transition velocities, New hybrid index, Pressure fluctuations,

Author affiliations:

[1]Institute of Chemical Engineering, Polish Academy of Sciences

Baltycka Street No. 5, 41-100 Gliwice, Poland

[2]Chair of Imaging Techniques in Energy and Process Engineering, Technische Universität Dresden, 01062 Dresden, Germany

[3]Institute of Fluid Dynamics, Helmholtz-Zentrum Dresden-Rossendorf,

Bautzner Landstraße 400, 01328 Dresden, Germany

[4]Chair of Chemical Process Engineering, Technische Universität Dresden, 01062 Dresden, Germany

[5]Institute of Process Engineering, Johannes Kepler University Linz, Altenbergerstr. 69, 4040 Linz, Austria

[*] Corresponding author. Email address: sned@iich.gliwice.pl

1 Introduction

Bubble columns (BCs) are used extensively in petrochemistry, biochemistry, waste water treatment, flotation, etc. The degrees of mixing, mass and heat transfer in these gas-liquid contactors depend on the prevailing flow regime (FR). Liquid movement and bubble properties (bubble size distribution (BSD), liquid circulation, two-phase structures, etc.) as well as the mode of gas-liquid interaction are much different in the main FRs [1]. The successful identification of the FR transitions is important for the modelling and simulation of the BC hydrodynamics as well as design and optimization of BC performance. Many different methods and approaches for FR identification have been reported in the BC literature. Summary of these methods is available in Nedeltchev et al. [2,3]. However, the new FR identifiers are not universal and they yield positive results only when they are applied to a specific signal (pressure, gas holdup, etc.).

There are three main FRs in BC operation. Each FR transition is related to the flow stability in the bubble bed [1]. The flow structure is complicated and it is associated with the bubble shape

oscillations, bubble wake formation and bubble path instability. The homogeneous FR is characterized with small bubbles (spherical and ellipsoidal), narrow bubble size distribution (BSD), gentle mixing, relatively flat radial gas holdup and liquid velocity profiles. The main parameters exhibit strong dependence on the type of gas distributor. The heterogeneous FR is characterized by two bubble classes (ellipsoidal and spherical-cap bubbles), wider BSD, parabolic radial gas holdup and liquid velocity profiles, existence of liquid circulation loops and negligibly small dependence of the main parameters on the gas distributor type. The transition from a homogeneous FR to heterogeneous FR is a gradual process.

One of the most important parameters in the BC operation are gas holdup and BSD. For every gas distributor, these two parameters together with the initial bubble size are quite specific and can be determined by means of modern measurement methods. Both parameters are very important for the BC reactor design and they affect significantly the mass transfer efficiency. Paul and Pakzad [4] argued that bubble wakes, bubble coalescence and breakage and liquid vortices result in a heterogeneous spatial-temporal distribution of bubble size and gas holdup. Numerous empirical correlations [5,6] for gas holdup prediction have been proposed. The radial profiles of gas holdup and BSD are governed largely by the gas distributor [7].

Both gas holdup and BSD depend on the superficial gas velocity U_g, which is a key operational parameter. The BSD changes gradually from uniform, narrow and monomodal in the homogeneous FR to bimodal having large bubbles in the heterogeneous FR [4]. The boundaries of the main FRs depend strongly on U_g and thus they define the regime-specific degrees of liquid mixing, turbulence and mass and heat transfer. The gas flow rate injected through the gas distributor governs the flow pattern in the bubble bed and the rising trajectory of bubbles. The main transition velocity (marking the end of the homogeneous FR) is a very important parameter since it is used for the calculation of both the large bubble diameter and large bubble holdup [8], which are key characteristics of the heterogeneous FR.

The gas phase can be regarded as a collection of discrete bubble sizes [4]. There is an excessive coalescence at higher U_g values, which results in is a characteristic bimodal BSD at higher U_g values [4]. The frequency of the smaller bubbles decreases. In other words, there is an increased flow homogeneity [4]. In many cases the gas holdup increases axially.

Joshi et al. [9] have applied the linear stability theory in order to model the main FR transition in BCs. A sophisticated time series analysis (for instance nonlinear chaos analysis or fractal analysis) is capable of extracting hidden information in any time series. Some researchers [2,3,10,11] have employed both statistical and chaotic methods as well as information entropy theory to analyze various time series in order to identify the boundaries of the main FRs. Most frequently pressure fluctuations are used, which characterize the motion of the gas bubbles in the gas-liquid dispersion. However, the pressure fluctuations contain certain degree of stochastic noise, which can lead to artificial disturbances in the profile of any complex parameter. Such strong sporadic disturbances can be observed in the work of Lin et al. [10]. This underpins the need for parameters, which are less sensitive to noise in the signal and allows easier interpretation of their profiles as a function of superficial gas velocity U_g.

Ruzicka et al. [12] reported the existence of a dual effect of liquid viscosity on the main FR transition. In the case of moderate viscosity (3-22 mPa·s) the homogeneous FR is destabilized and the main transition occurs earlier. On the other hand, the low viscosity (1-3 mPa·s) stabilizes the homogeneous FR. Ruzicka et al. [13] reported also a dual effect of surface tension on the regime transition. Yang et al. [1] argue that the critical bubble diameter varies gently with surface tension but it is highly influenced by liquid viscosity.

Several research groups have used alcohols in their research. Zahradnik et al. [14] studied the effect of addition of alcohols on gas holdups in aqueous saccharose solutions. Krishna et al. [15,16] investigated also the influence of alcohol addition on gas holdup profiles. A scale-up model has been developed. Nedeltchev et al. [2,3] and Krishna et al. [17] identified the main transition

velocity in BCs operated with nitrogen-ethanol and air-ethanol systems. In the current work, this research will be extended to aqueous solutions of alcohols (ethanol and iso-propanol).

In the current work, the main novelty is associated with the definition of a new parameter (called new hybrid index (NHI)) for flow regime identification. The NHI definition (see section 2) implies that two sub-parameters should be considered in order to compare their behaviour over a certain period. In such a way, the local minimum in the new parameter will distinguish the most structured ("non-chaotic" according to [11]) flow pattern, which corresponds to the main transition (critical) velocity. The post-processing strategies of the time-dependent signal are also clearly presented. The newly defined parameter is based on collected information from all parts of the signal, which covers a relatively long time period. In such a way, if there is a small instability (disturbance) in the system for a short time, then the new parameter will take into account this change in the operating conditions. In summary, the new parameter extracts new hidden information that can be useful for FR identification. It will be demonstrated the new sophisticated parameter is applicable to various different types of signals. In addition to the NHI definition, this work reports the main transition velocities in new gas-liquid systems, which are not very well studied, namely mixtures of deionized water and alcohols.

1.1 Previously developed identification parameters in bubble columns

The most important articles focused on FRI in BCs have been summarized recently in [2,3]. The most reliable identifiers of the main transition (critical) velocities are those based on sophisticated signal reconstructions. In general, this means splitting the signal into different parts and comparison of their growing differences with time. Table 1 summarizes the most important parameters based on various signal reconstruction techniques. Most of these methods are mainly capable of identifying accurately the first (main) transition velocity.

Table 1. Overview of the various identification parameters in bubble columns.

Parameter	Theory	Brief description	Literature source
Kolmogorov entropy (KE)	Chaos	Characterizes the information loss in a chaotic system	Lin et al. [10], Letzel et al. [11], Nedeltchev et al. [19,20]
Correlation dimension	Chaos	Quantifies the complexity of chaotic attractors	Lin et al. [10], Letzel et al. [11]
Lyapunov exponents	Chaos	Characterizes the exponentially divergent rate of two nearby orbits	Lin et al. [10]
Fractal dimension	Fractal analysis	= 2-Hurst exponent; This parameter measures how complicated a self-similar figure is	Lin et al. [10]
Hurst exponent	Rescaled range analysis	Higher values of Hurst exponent indicate more persistent data exhibiting some trends	Kikuchi et al. [21]
Mann-Whitney statistic	Statistical analysis	Lower value indicates a significant deterministic component in the time series	Kikuchi et al. [21]
Mutual information with a zero time delay	Information	No clear definition	Lin et al. [10]
Information entropy	Information	Characterizes the amount of information contained in every signal	Nedeltchev et al. [19]
Shannon entropy	Information, Probability	Measures the amount of information and degree of indeterminancy in a certain source	Nedeltchev et al. [22] Zhong et al. [23]
Degree of randomness	Information, chaos	Characterizes the degree of randomness in the signal	Nedeltchev et al. [24]

New statistical parameter	Statistical	Characterizes the signal's homogeneous distribution between minimum and maximum values	Nedeltchev et al. [25]

The other methods without signal reconstruction involve calculation of average absolute deviation (AAD) [2], average cycle time [20], drift flux [26], etc. These simple methods are capable of identifying only the first transition (critical) velocity.

2 Derivation of the new hybrid index (NHI)

A novel dimensionless parameter called new hybrid index (NHI) has been developed in this work. The most important first step in the NHI calculation is the division of time series into different intervals consisting of at least 500 data points (exceeding 2-3 gas recirculation times). In such a way, the structure of the time series will be taken into account. Due to the gas supply instabilities the degree of turbulence and inhomogeneity in the time series is different in the different intervals. In this work, the electrical resistivity tomographic (ERT) data (30,000 points) will be divided into six intervals consisting of 5,000 points. The aerated height time series (4,000 points) will be divided into 8 intervals consisting of 500 points. Both differential pressure (DP) and gauge pressure (GP) fluctuations (10, 000 points) will be divided into 10 periods consisting of 1,000 points. The second step in the NHI algorithm is to calculate the average absolute deviation (AAD) in each data interval. AAD is a robust statistical estimator of the data width around the mean. It is a sum of all absolute differences $|x_j\text{-}x_{mean}|$ divided by the total number of points in the time series. For the first time, it has been used for FR identification by Lin et al. [10].

Further, the probability P_i that a certain data interval yields a particular AAD will be calculated as the ratio of the AAD in that interval divided by the sum of all AAD values as:

$$P_i = AAD_i / \sum_{i=1}^{N} AAD_i \,. \quad (1)$$

N is the number of the equal intervals, into which the time series are divided.

Following the information entropy theory [2], the information amount IA_i in each interval will be calculated as:

$$IA_i = -\log(P_i) . \quad (2)$$

The new hybrid index (NHI) represents the ratio:

$$NHI = |\sum_{i=1}^{N} IA_i - \sum_{i=1}^{N} AAD_i| / \sum_{i=1}^{N} IA_i . \quad (3)$$

U_g values below 0.015 m/s result in NHI>>1. This effect is attributable to the gas maldistribution in the bubble bed. However, at $U_g \geq 0.025$ m/s, NHI varies between 0 and 1.

The NHI parameter extracts useful hidden information (difference between information amount and statistical deviation from the signal's mean) from the time series and characterizes the statistical non-uniformity in the measured time-dependent signal. As other researchers [11] argued, at the main transition velocity (end of the homogeneous FR) the signals are better ordered, i.e. statistically more uniform.

The new parameter NHI quantifies the difference between two important quantifiers, namely information amount (IA) and summed average absolute deviation (AAD). When this difference is very small, then we have a very ordered flow pattern (structure) and this is the definition of the main regime transition velocity [11]. So, when the NHI values are high we have a low order in the flow pattern and when the NHI values are low we have a well-ordered flow structure. It is advantageous that most of the values of the new parameter NHI vary in the range of 0-1 and their physical meaning could be clearly understood. Unity corresponds to maximum difference between statistical and information sub-parameters and zero corresponds to perfectly ordered flow pattern and signal. The new parameter smoothly changes between different operating conditions belonging to the same FR.

In this work a useful division scheme for every signal processed is presented. All reported positive results in section 4 are based on the specific divisions explained in every sub-section. Such an arbitrary division has also been used in the Komogorov entropy (KE) algorithm [11] where numerous random vector pairs have been generated. The selection of the division scheme in the

current work is more or less arbitrary provided that in every interval there are at least 500 points (minimum 2-3 gas recirculation times), which guarantee that sufficient statistical information will be obtained. In the current work the first transition velocities identified on the basis of the proposed division scheme are well predictable by a frequently used semi-empirical correlation.

3 Experimental Setups

Various time-dependent signals (characterizing the BC hydrodynamics) have been recorded in different BC facilities (different clear liquid heights, gas distributor layouts, etc.) in order to demonstrate that new parameter is universally applicable. Different gas-liquid systems have also been investigated.

3.1 Measurements with Electrical Resistivity Tomography (ERT)

The BC consisted of vertically installed glass pipe sections with an inner diameter (ID) of 0.1 m and a total height of 1.65 m. A schematic of the experimental setup is depicted in Fig. 1.

Air is provided from the compressed air supply. The superficial gas velocity U_g is adjusted with a mass flow controller (MFC) from Brooks Instrument® (GF040 series). Gas enters the column via a cross-sparger, which is positioned 0.05 m above the bottom of the column with the drillings facing the bottom. The sparger has 4 legs with 3 drillings in each leg (cf. Fig. 1, right side). The column was filled with tap water up to an initial filling height of 1.05 m, so that the water level L_0 was 1.0 m above the gas sparger.

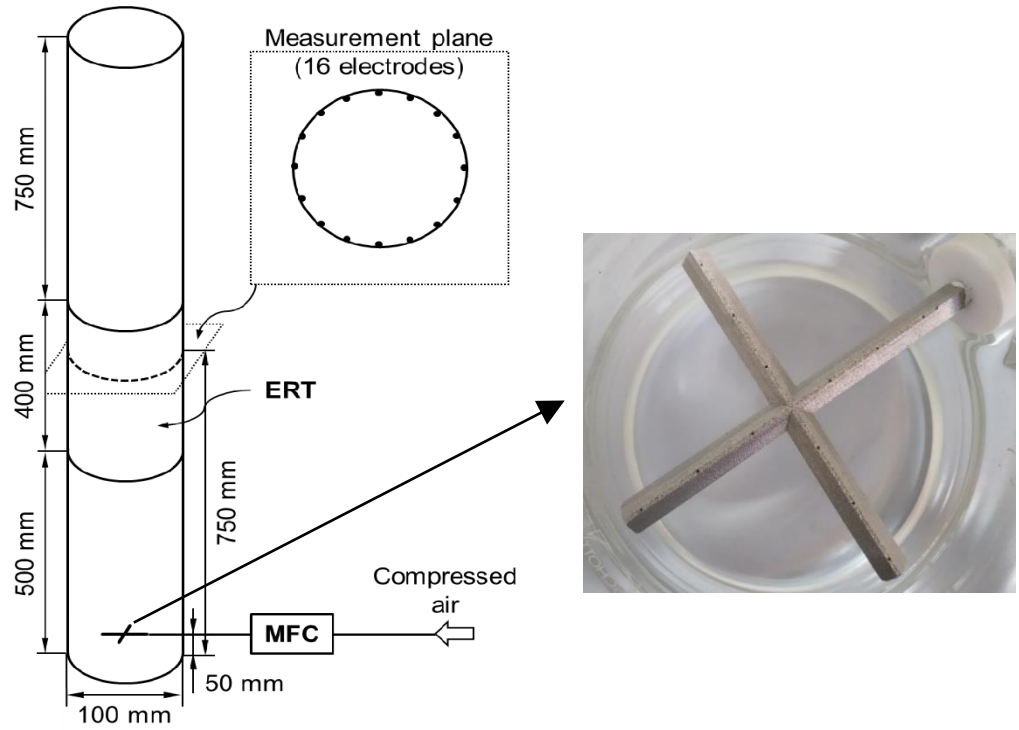

Figure 1. Experimental setup for the ERT measurements (left) and photography of the used cross-sparger (right).

An ERT sensor (Industrial Tomography Systems, ITS) is mounted in the middle of the column. The sensor contains a measurement plane 0.7 m above the gas sparger with 16 electrodes in a circular arrangement. The electrodes of the ERT sensor are in contact with the conductive liquid and are embedded in a PEEK liner. The whole ERT sensor is built into a housing of stainless steel. The electrodes are connected to the data acquisition system v5r manufactured by ITS. The system can be also found in literature for measurements in various multiphase FRs [27,28].

The measurement procedure of the ERT system can be imagined by an excitation of one pair of electrodes while the voltage between other electrode pairs is measured. The excitation and measurement sequences follow the adjacent strategy [29]. With this strategy voltage is injected into a pair of neighboring electrodes and simultaneously the current is measured. Then voltage is measured in sub-sequential adjacent electrode pairs. The procedure is repeated until all independent measurements are taken. From each run a cross-sectional image can be reconstructed. A reference measurement with the unaerated liquid is taken to calibrate the voltage signals. As a continuous

phase tap water was used and a conductivity of $\sigma_1 = 160\,\mu S/cm$ was measured with the Seven2Go™ Pro Conductivity Meter S7 from Mettler Toledo.

For the reconstruction of the cross-sectional conductivity images the non-iterative reconstruction algorithm Modified Sensitivity Back-Projection was used [30]. From the conductivity tomograms cross-sectional images for the gas volume fraction α can be calculated with Maxwell's equation [31]:

$$\alpha = \frac{2\sigma_1+\sigma_2-2\sigma_{mc}-\frac{\sigma_{mc}\sigma_2}{\sigma_1}}{\sigma_{mc}-\frac{\sigma_2}{\sigma_1}\sigma_{mc}+2(\sigma_1-\sigma_2)}, \tag{4}$$

where σ_1 is the conductivity of the continuous phase and σ_{mc} is the conductivity of the mixture. For a non-conductive dispersed phase, $\sigma_2 = 0$ and Eq. (4) simplifies to

$$\alpha = \frac{2\sigma_1-2\sigma_{mc}}{\sigma_{mc}+2\sigma_1}. \tag{5}$$

For every superficial gas velocity 100,000 frames were recorded with a frequency of 315 Hz. The superficial gas velocity U_g was varied from 0.01 up to 0.12 m/s in steps of 0.005 m/s. In this work the time series of the center pixel of the column are used for the FR analysis. The total duration of a single measurement for one operating point was 315 seconds.

3.2 Monitoring of the aerated height changes with time

The time-dependent measurements of the aerated liquid height L (also called bubbling bed height) are important in order to approximate the gas holdup fluctuations. In this work, the L time series have been obtained based on a buoyancy device installed vertically downwards on a rod. The lowest point of the buoyancy probe was fixed at 0.535 m. This value determines the lowest clear liquid height that can be used. When U_g increases and the bubble bed becomes more aerated, the buoyancy device rises along with the bubble bed surface and instant values of L are recorded. The buoyancy device has been made of stainless steel. The sampling frequency has been set at 25 Hz. The measurements have been performed in an acrylic BC (0.1 m in ID) operated with an air-

deionized water system at ambient conditions. In the first case, a perforated plate (PP) gas sparger (85 orifices × Ø 1.0 mm, open area (OA) = 0.85%) has been used. By means of an additional porous plate below the gas sparger, a uniform gas distribution has been ensured. Without this porous plate, a detrimental gas maldistribution was observed at low U_g . The clear liquid height L_0 was fixed at 1.0 m. The aerated height L fluctuations have been treated by the new NHI algorithm in order to identify precisely the main FR boundaries.

3.3 Measurements with differential pressure transducers

The differential pressure (DP) fluctuations have been performed in a stainless steel BC (0.102 m in ID; height: 2.4 m) operated with a nitrogen-ethanol (96 %) system at ambient conditions. The column has been equipped with a PP gas distributor (19 orifices × Ø 1.0 mm). The DP time series have been recorded at a sampling frequency of 100 Hz. One leg of the DP transducer (LABOM GmbH, Germany, range 0–1 bar) was connected to an axial position of 0.65 m, whereas the other end of the DP transducer was connected (by a common pipe) to the column top.

This pressure technique is nonintrusive since both ends of the DP sensor are mounted at the outer side of the column wall. Again, a PP gas distributor (19 orifices × ∅ 1.0 mm) was used. The U_g range varied from 0.01 to 0.1 m/s.

3.4 Measurements with gauge pressure transducers

Gauge pressure (GP) fluctuations have been recorded in an acrylic BC (0.1 m in ID) with a sampling interval of 30 ms by means of a GP transmitter PR-33X (Range: 0-1 bar) manufactured by Keller AG (Switzerland). The column has been equipped with a PP gas distributor (93 orifices × Ø 1.0 mm). GP measurements were performed at an axial height of 0.65 m above the gas distributor. The clear liquid height L_0 was fixed at 1.1 m. All pressure measurements were performed with an error of ± 5 %. The GP measurements were conducted in two aqueous solutions of alcohols: deionized water + ethanol (0.5 wt. %) and deionized water + iso-propanol (0.5 wt. %).

The physicochemical properties of these mixtures were measured (see Table 2) in our research group.

Table 2. Physicochemical properties of ethanol and aqueous solutions of alcohols used.

Liquid	**Viscosity [mPa s]**	**Density [kg m^{-3}]**	**Surface tension [N/m]**
Ethanol (96 %)	1.24×10^{-3}	793	22.1×10^{-3}
Deionized water + 0.5 wt. % ethanol	0.918×10^{-3}	996.832	69.693×10^{-3}
Deionized water + 0.5 wt. % iso-propanol	0.925×10^{-3}	996.792	67.388×10^{-3}

4 Results and discussion

4.1 Similarity in the behavior of the NHI profiles extracted from ERT data, aerated height fluctuations and DP data in BCs (0.1 m in ID) operated with both air-water and nitrogen-water systems

Fig. 2a shows that the well-pronounced local minimum in the NHI profile (extracted from ERT data) is capable of identifying the main (first) transition (critical) velocity $U_{trans-1}$ in an air-deionized water BC (0.1 m in ID, cross sparger, 12 orifices × ∅ 1.0 mm) at 0.045 m/s. It is an important merit that the $U_{trans-1}$ value is clearly and straightforwardly identified. The local NHI minimum means that the difference between total IA and total AAD is the lowest, i.e. this measurement is characterized with the highest degree of order, which is the definition of FR transition [11]. It is noteworthy that this critical gas velocity is very close to the value of 0.047 m/s reported as a "second transition point" by Ajbar et al. [32]. The researchers used a BC (0.15 m in ID) equipped with a ring-sparger with six legs (star-like cross) with 85 orifices × ∅ 1.0 mm. A well-pronounced local Kolmogorov entropy (KE) minimum has been observed at this critical gas velocity. It should also be noted that the main transition velocity identified in Fig. 2a is very close to the prediction (0.048 m/s) of Im et al. [25]. Based on simulations, Wang et al. [33] have shown that the transition velocity for an air-water system occurs at 0.04 m/s. Gas distributor type and column diameter have

not been specified. Nedeltchev et al. [20] have identified the $U_{trans-1}$ value (based on KE profile) at 0.04 m/s for a BC (0.1 m in ID) equipped with a PP gas distributor (64 orifices × ∅ 1.32 mm). Nedeltchev et al. [20] has confirmed this transitional velocity in an air-water BC (0.1 m in ID) equipped with another type of PP gas sparger (55 orifices × ∅ 0.5 mm).

At U_g = 0.08 m/s the NHI profile levels off and this point distinguishes the onset of the heterogeneous FR. In between the two U_g boundaries exist the transition FR. It is noteworthy that similar criteria as the ones applied to the NHI profile (see Fig. 2a) have been used by Lin et al. [10] in order to interpret their mutual information at zero time delay.

When the NHI profile is extracted from aerated height L fluctuations recorded in an air-deionized water BC (0.1 m in ID, PP gas distributor, 85 orifices × ∅ 1.0 mm) by means of a buoyancy device, then the same well-pronounced drop (almost equal to zero) in the NHI values (see Fig. 2b) is observed, however, at a lower U_g value (0.032 m/s). Obviously, the usage of a cross sparger (in the case of ERT data) stabilizes the homogeneous FR. A comparison between the results in Figs. 2a-b reveal that the PP gas distributor shifts the transition velocities to lower U_g values. The $U_{trans-1}$ value is very close to the prediction (0.029 m/s) of the empirical correlation of Reilly et al. [34]. For comparable number of orifices and orifice diameter (85 orifices × ∅ 1.0 mm), Ajbar et al. [32] identified the first transition velocity at 0.027 m/s. The researchers have used ring-sparger with six legs (star-like cross). It is noteworthy that the second transition velocity $U_{trans-2}$ is very close to the prediction (0.048 m/s) of another correlation [26].

Beyond 0.032 m/s follows a steep increase (see Fig. 2b) in the NHI values, which is characteristic for the transition FR. At U_g = 0.046 m/s the NHI profile levels off. This critical gas velocity distinguishes the onset of the heterogeneous FR.

In case of the nitrogen-tap water system aerated in a BC (0.102 m in ID) equipped with a PP distributor (19 orifices × ∅ 1.0 mm), the NHI parameter (extracted from DP fluctuations) is capable of identifying clearly two main transition velocities. Fig. 2c shows the first well-pronounced NHI

minimum occurs at U_g=0.029 m/s exactly as predicted by the correlation of Reilly et al. [34]. Vial et al. [35] supported this finding in the case of an effective gas distributor. Based on the information entropy, Nedeltchev and Shaikh [2] have identified the $U_{trans-1}$ value at 0.025 m/s. In Fig. 2c the second well-pronounced NHI minimum is observable at U_g=0.047 m/s. This critical gas velocity is predictable by means of the empirical correlation of Im et al. [26].

Additional support for the successful identification of the main transition velocity in Fig. 2a can be provided by considering the gas holdup profile. Fig. 3 shows that the gas holdups up to 0.045 m/s can be approximated by a straight line. Beyond 0.045 m/s the rate of increase of the gas holdup changes and this point distinguishes the end of the homogeneous FR. In other words, the results about $U_{trans-1}$ from Figs. 2a and 3 coincide. The other gas holdup profiles exhibit the same trends.

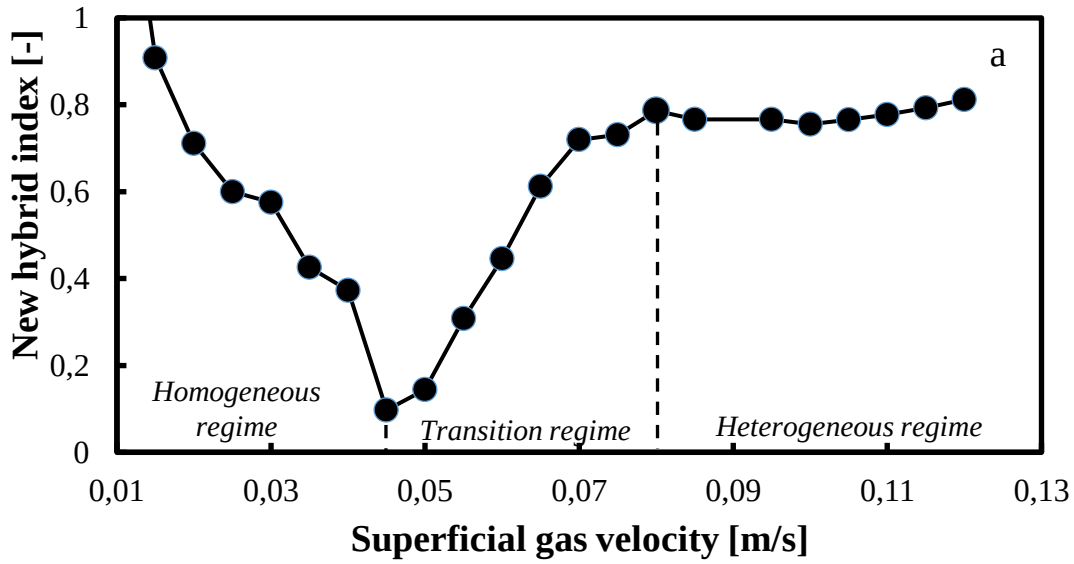
a
New hybrid index [-]
1
0,8
0,6
0,4
0,2
0
Homogeneous regime
Transition regime
Heterogeneous regime
0,01
0,03
0,05
0,07
0,09
0,11
0,13
Superficial gas velocity [m/s]

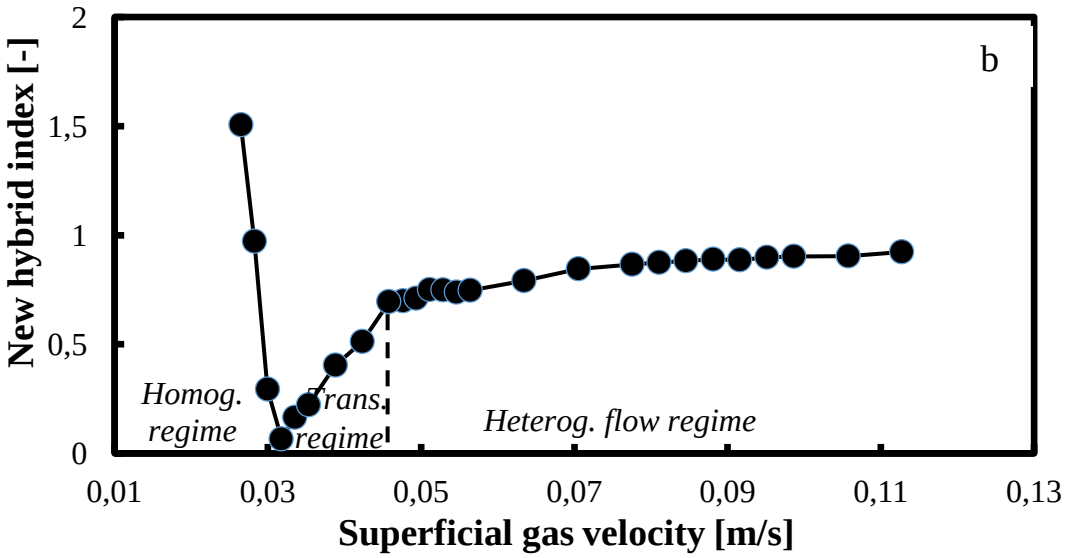
b
New hybrid index [-]
2
1,5
1
0,5
0
Homog. regime
Trans. regime
Heterog. flow regime
0,01
0,03
0,05
0,07
0,09
0,11
0,13
Superficial gas velocity [m/s]

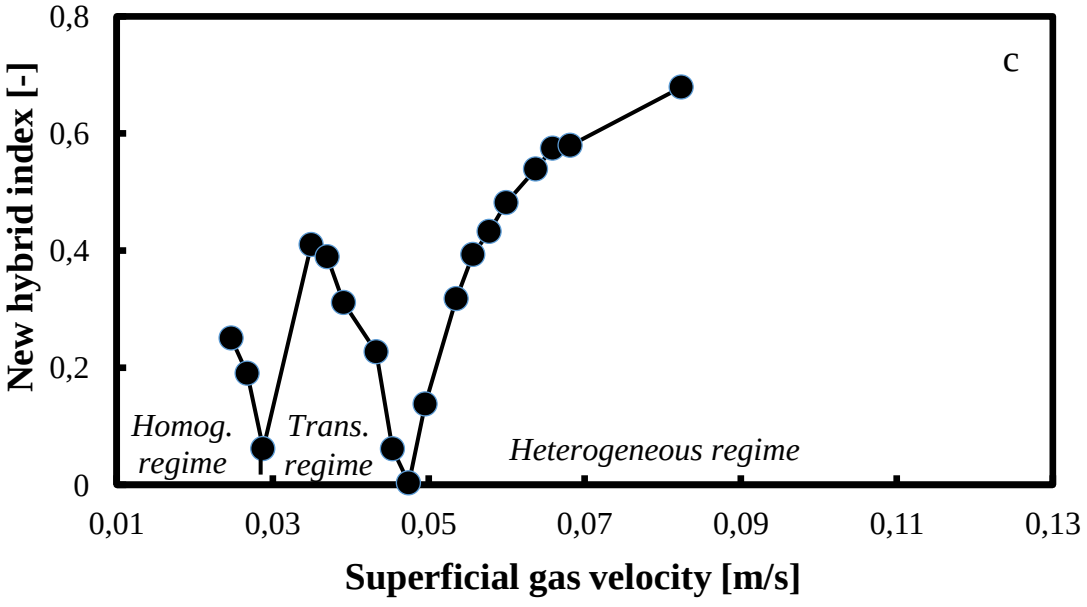
c
New hybrid index [-]
0,8
0,6
0,4
0,2
0
Homog. regime
Trans. regime
Heterogeneous regime
0,01
0,03
0,05
0,07
0,09
0,11
0,13
Superficial gas velocity [m/s]

Figure 2. FR boundaries identified by means of the NHI values extracted from: (a) ERT data in a BC (0.1 m in ID) operated with an air-deionized water system (L_0=1.0 m); (b) aerated height fluctuations in a BC (0.1 m in ID) operated with an air-deionized water system (L_0=1.0 m); (c) DP fluctuations in a BC (0.1 m in ID) operated with a nitrogen-tap water system (L_0=1.3 m).

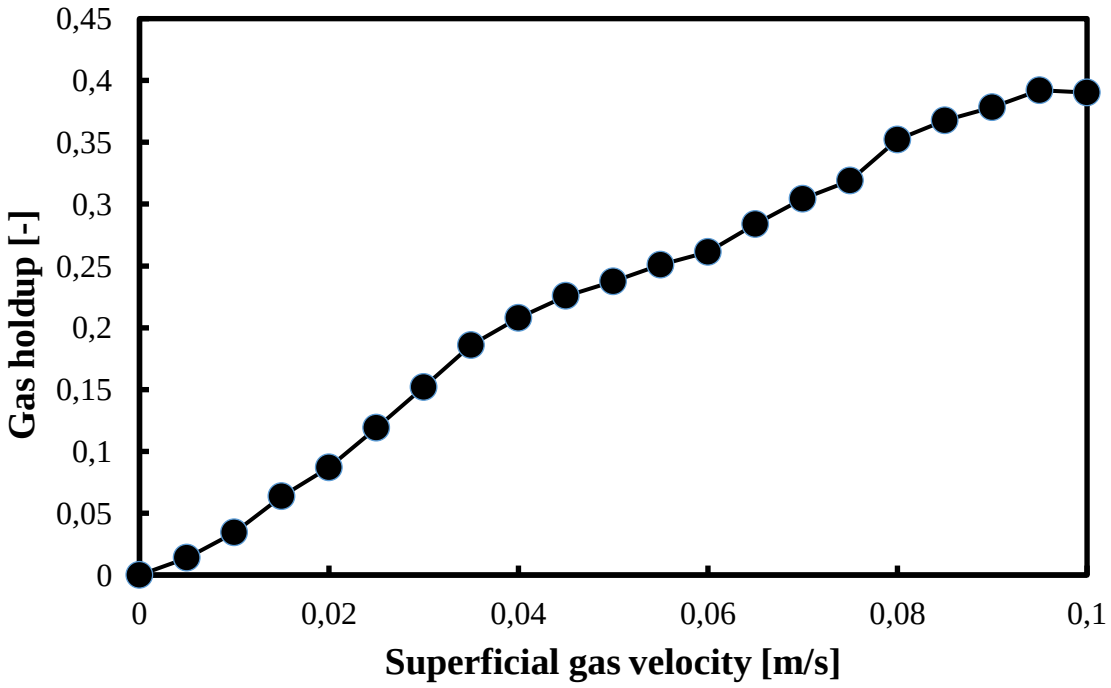

Figure 3. Gas holdup profile recorded by an ERT facility in an air-water BC (0.1 m in ID) equipped with a cross-sparger 12 orifices × ∅ 1.0 mm).

4.2 NHI results in an ethanol-nitrogen system and an aqueous solution of ethanol-air system

Fig. 4a shows that when pure ethanol is aerated with nitrogen in a BC (0.102 m) equipped with a PP gas distributor (19 orifices × ∅ 1.0 mm), the NHI profile is similar to the case of air-water system (see Figs. 2a,b). At U_g=0.028 m/s a well-pronounced local NHI minimum is observed. It identifies the end of the homogeneous FR. Krishna et al. [17] reported a main transition velocity of 0.027 m/s in a narrow BC (0.05 m in ID) equipped with a porous plate gas distributor (20-40 μm). It is noteworthy that the correlation of Reilly et al. [34] predicts the value of 0.026 m/s for $U_{trans-1}$. The second transition velocity $U_{trans-2}$ is not identifiable by a local NHI minimum. As it was mentioned before, it should be assumed that the onset of the heterogeneous FR is the U_g value at which the NHI profile practically levels off. In this particular case, the $U_{trans-2}$ value is identifiable at 0.07 m/s (see Fig. 4a). Beyond this critical gas velocity, the NHI values slightly increase but with much slower rate.

The NHI parameter works well also in the case of measurements with a mixture of deionized water and ethanol (0.5 wt. %). Fig. 4b shows that again a well-pronounced minimum identifies the main transition velocity $U_{trans-1}$ (end of the homogeneous FR) at U_g=0.038 m/s. This critical gas velocity practically coincides with the one identified by Hyndmann et al. [36]. The usage of alcoholic solutions stabilizes the homogeneous FR due to the suppression of coalescence [37,38]. The stabilization of the homogeneous FR by the addition of ethanol has been confirmed by Krishna et al. [15-17] and Al-Oufi et al. [39]. Besagni et al. [40] reported also that the addition of ethanol in a large BC stabilizes the homogeneous FR, increases gas holdup and bubble shapes as well as widens the BSD.

It is noteworthy that the measurements in Fig. 4b started at U_g=0.03 m/s since a gas maldistribution was observed at lower U_g values. The transition FR was stable up to U_g=0.073 m/s, where the NHI value was practically zero. This critical gas velocity is similar to the one identified in Fig. 4a. The heterogeneous FR is stable up to U_g=0.085 m/s. Beyond this threshold U_g value a regime of complete foaming is established.

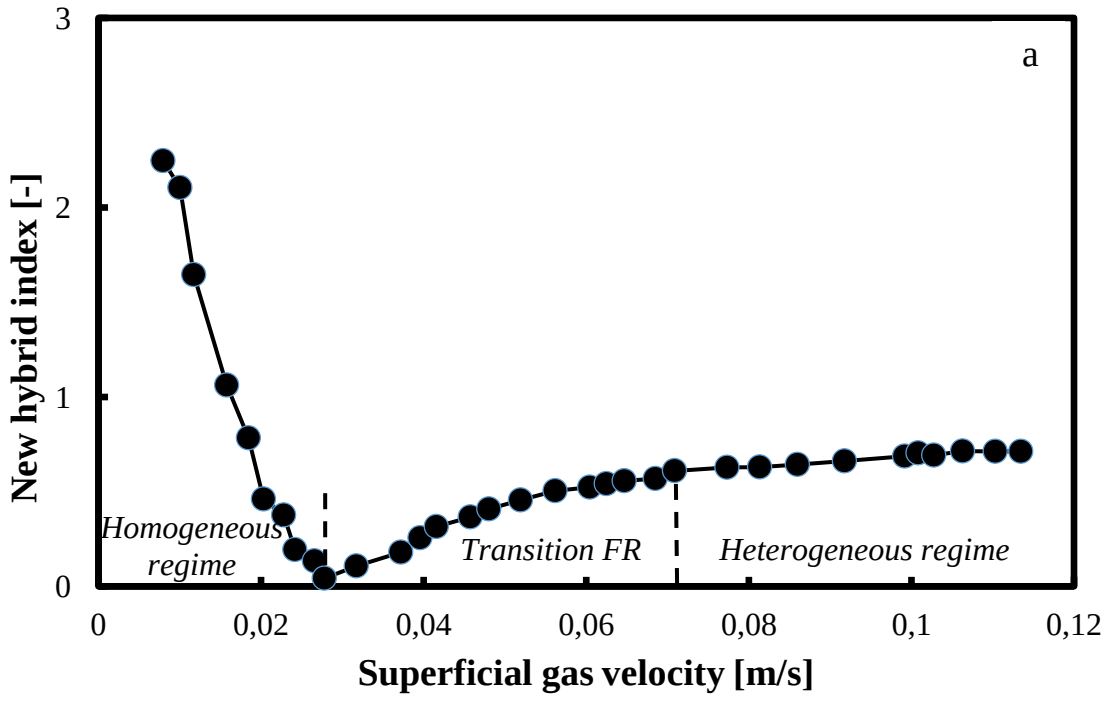

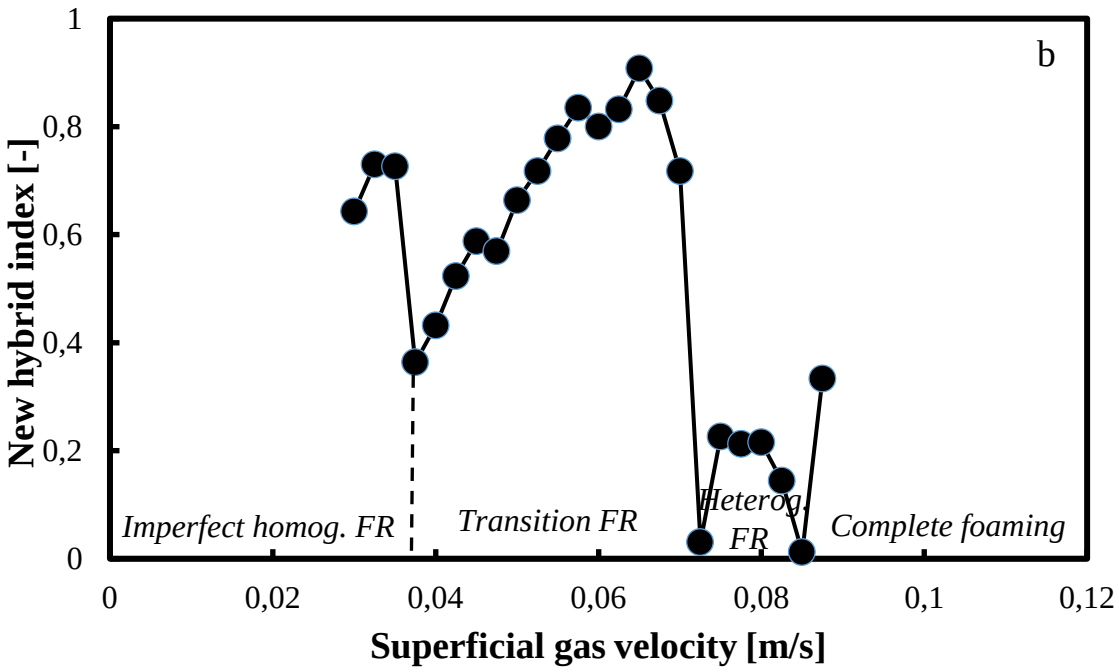

Figure 4. FR boundaries identified by means of the NHI values extracted from: (a) DP fluctuations in a BC (0.1 m in ID) operated with a nitrogen-ethanol system (L_0=1.3 m); (b) GP fluctuations in a BC (0.1 m in ID) operated with air and an aqueous solution of ethanol (deionized water + 0.5 wt. % ethanol) (L_0=1.1 m).

It is noteworthy that for this particular liquid mixture the heterogeneous FR is related to the enhanced liquid turbulence (due to multiple liquid circulation loops) in the column and not related to bubble coalescence. Large spherical-cap bubbles were not observed visually in the bubble bed. The two small NHI minima in the transition FR should be neglected since they are very small drops in comparison with the other well-pronounced local NHI minima. It is advantageous that the NHI profile is capable of identifying the onset of complete foaming, which is not effective for the BC operation and thus it should be avoided.

4.3 NHI results in aqueous solution of iso-propanol (0.5 wt. %)

When an aqueous solution of iso-propanol (0.5 wt. %) is aerated with air, the local NHI minima are not so deep. Fig. 5 shows that a small local minimum at U_g=0.033 m/s identifies the end of the imperfect homogeneous FR. The characteristics of this hydrodynamic regime are described in Leonard et al. [41]. Usually, when the bubbles are smaller, then the sudden changes in the NHI

values are not so pronounced. At U_g = 0.058 m/s another local minimum is observed. It distinguishes the end of the transition FR. This critical gas velocity is much lower than the one in Fig. 4b. The heterogeneous FR is stable up to U_g = 0.070 m/s and then the regime of complete foaming begins.

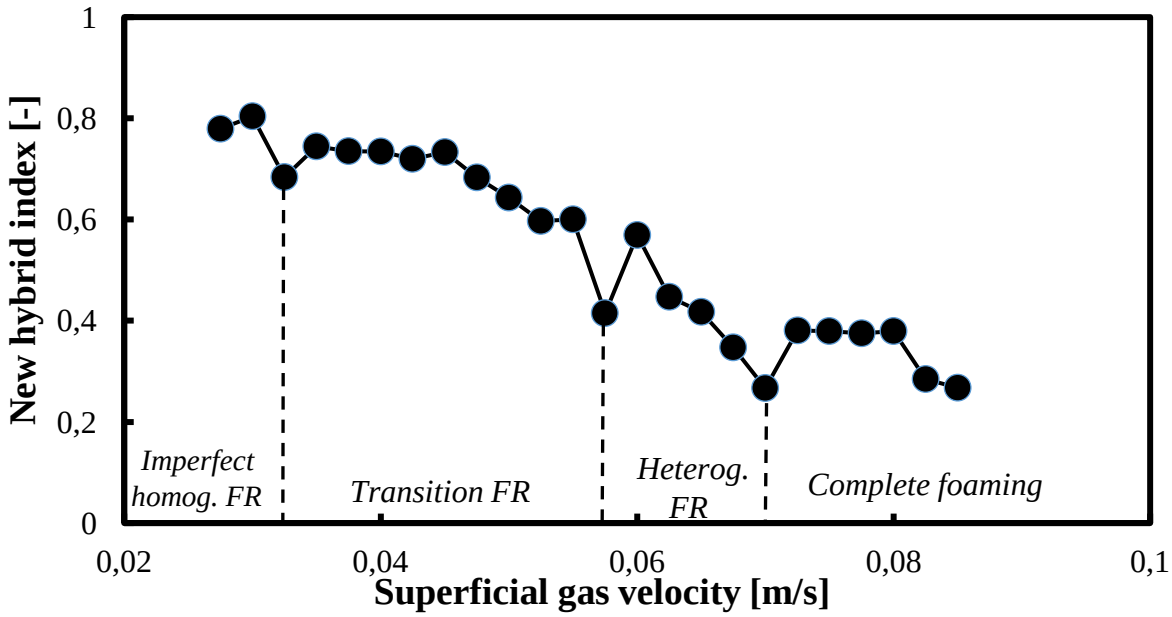

Figure 5. FR boundaries identified by means of the NHI values in an aqueous solution of iso-propanol (deionized water + 0.5 wt. % iso-propanol) aerated in a BC (0.1 m in ID, L_0=1.1 m).

In summary, the main transition velocity $U_{trans-1}$ is clearly identifiable on the basis of the well-pronounced local minimum in the NHI profile. Such a criterion has been used by Nedeltchev et al. [2,3], Lin et al. [10] and Letzel et al. [11]. All these researchers demonstrated that the gas-liquid dispersion is well ordered (structured) and its behavior is fully predictable especially at the main transition velocity $U_{trans-1}$. The local NHI minimum always occurs in between 0.03 m/s and 0.04 m/s. The data show that it slightly depends on the type of the gas distributor used. When aqueous solutions of alcohols are used, then $U_{trans-1}$ value shifts to lower U_g values in case of smaller gas bubbles.

Table 3 summarizes the comparisons between the main transition velocities identified in this work and the predictions of the two available empirical correlations in the literature. A conclusion could be drawn that when a PP distributor is used, then the differences between experimentally

identified transition velocities and theoretically predicted ones are minimal. Under these conditions the correlation of Reilly et al. [34] is applicable. On the other hand, when a ring-sparger (ERT data) is used, then the main transition velocity $U_{trans-1}$ is predictable by the correlation of Im et al. [26]. These results imply that the semi-empirical correlations are still not very effective and the experimental determination of the main transition velocities based on new reliable reconstruction methods is the preferable approach in order to avoid serious miscalculations for the FR boundaries.

Table 3. Summary of the identified main transition velocities and comparison with the predictions of the widely used semi-empirical correlations in the literature.

Measurement type	**Experimental $U_{trans-1}$ and $U_{trans-2}$ [m/s] (Figure #)**	**Emp. $U_{trans-1}$ [m/s] Reilly et al. [34]**	**Emp. $U_{trans-1}$ [m/s] Im et al. [26]**
ERT data (air-tap water)	0.045 (see Fig. 2a) 0.08 (see Fig. 2a)	0.029	0.048
Gas holdup data (air-deionized water)	0.032 (see Fig. 2b) 0.046 (see Fig. 2b)	0.029	0.048
DP data (nitrogen-tap water)	0.029 (see Fig. 2c) 0.047 (see Fig. 2c)	0.029	0.048
DP data (nitrogen-ethanol)	0.028 (see Fig. 4a) 0.07 (see Fig. 4a)	0.038	0.037
GP data (air-aqueous soltn. of ethanol (0.5 wt. %))	0.038 (see Fig. 4b) 0.073 (see Fig. 4b)	0.029	0.049
GP data (air-aqueous soltn. of iso-propanol (0.5 wt. %))	0.033 (see Fig. 5) 0.058 (see Fig. 5)	0.029	0.048

5 Conclusions

A new reliable parameter (called new hybrid index - NHI) for FRI in various BCs has been successfully developed. It has been found that this universal parameter works well with ERT data, gas holdup fluctuations, differential pressure (DP) and gauge pressure (GP) time series. The data

were recorded not only in an air-water system but also in a nitrogen-ethanol and aqueous solutions of alcohols (ethanol and iso-propanol). The end of the homogeneous FR was always identified by means of a local well-pronounced NHI minimum. In many cases, the onset of the heterogeneous FR was identified as the critical gas velocity, at which the NHI profile levels off. One of the main conclusions of this work is that the first transition (critical) velocity $U_{trans-1}$ varies between 0.028 m/s and 0.045 m/s depending on the gas-liquid system and especially on the gas distributor type. The second transition velocity $U_{trans-2}$ varies from 0.046 m/s to 0.08 m/s. Again, $U_{trans-2}$ depends on the gas-liquid system and the type of the gas distributor used. In summary, the new parameter extracts useful hidden information in the time series that could be used for FR identification. By means of NHI profiles, a set of new transition velocities was obtained. It will be used further for the development of new empirical correlations for prediction of the main transition velocities and development of a modern FR map.

Acknowledgment

The funding of the Alexander von Humboldt Foundation (Germany) within the framework of the "Research Group Linkage Programme" (Ref 3.4-1117626-POL-IP) is gratefully acknowledged.

Symbols used

AAD	[– ; mbars]	average absolute deviation
IA	[bits]	information amount
L	[m]	aerated liquid height
L_0	[m]	clear liquid height
NHI	[-]	new hybrid index
N	[-]	number of pre-selected intervals
P	[-]	probability of obtaining a certain AAD value
U_g	[m/s]	superficial gas velocity

U_{trans}	[m/s]	transitional gas velocity
$U_{trans-1}$	[m/s]	first transitional gas velocity
$U_{trans-2}$	[m/s]	second transitional gas velocity
x	[– ; mbars]	single value in the recorded signal
x_{mean}	[– ; mbars]	mean value from the time series

Greek letters

α	[–]	gas volume fraction obtained from ERT data
ε_g	[–]	gas holdup
σ_1	[µS/cm]	conductivity of the continuous phase
σ_2	[µS/cm]	conductivity of the dispersed phase
σ_{mc}	[µS/cm]	conductivity of the mixture

Abbreviations

BC bubble column

BSD bubble size distribution

DP differential pressure

ERT electrical resistivity tomography

FR flow regime

FRI flow regime identification

GP gauge pressure

ID inner diameter

ITS Industrial Tomography Systems

KE Kolmogorov entropy

MFC mass flow controller

OA open area

PP perforated plate

References

[1] N. Yang, J. Chen, W. Ge, J. Li, *Chem. Eng. Sci.* **2010**, *65*, 517-526. doi:10.1016/j.ces.2009.06.014

[2] S. Nedeltchev, A. Shaikh, *Chem. Eng. Sci.* **2013**, *100*, 2-14.

[3] S. Nedeltchev, J. Katerla, E. Basiak, *J. Chem. Eng. Japan* **2022**, *55*, 201-216. doi:10.1016/j.cej.2006.08.027

[4] M. M. Paul, L. Pakzad, *Can. J. Chem. Eng.* **2022**, *100*, 3030-3046. DOI: 10.1002/cjce.24352

[5] A. Kemoun, B. C. Ong, P. Gupta, M. H. Al-Dahhan and M. P. Dudukovic, *Int. J. Multiphase Flow* **2001**, *27*, 929-946.

[6] S. Nedeltchev, A. Schumpe, *J. Chem. Eng. Japan* **2008**, *41*, 744-755.

[7] M. T. Dhotre, J. B. Joshi, *Chem. Eng. J.* **2007**, *125*, 149-163. doi:10.1016/j.cej.2006.08.027

[8] R. Krishna, J. Ellenberger, *AIChE J.* **1996**, *42*, 2627-2634.

[9] J. B. Joshi, N. S. Deshpande, M. Dinkar, D. V. Phanikumar, *Advances in Chemical Engineering*

2001, *26*, 1-130.

[10] T.-J. Lin, R.-C. Juang, Y.-C. Chen, C.-C. Chen, *Chem. Eng. Sci.* **2001**, *56*, 1057-1065.

[11] H.-M. Letzel, J. C. Schouten, R. Krishna, C. M. Van den Bleek, *Chem. Eng. Sci.* **1997**, *52*, 4447-4459.

[12] M. Ruzicka, J. Drahos, P. C. Mena, J. A. Teixeira, *Chem. Eng. J.* **2003**, *96*, 15-22.

[13] M. Ruzicka, M. M. Vecer, S. Orvalho, J. Drahos, *Chem. Eng. Sci.* **2008**, *63*, 951-967.

[14] J. Zahradnik, G. Kuncova, M. Fialova, *Chem. Eng. Sci.* **1999**, *54*, 2401-2408.

[15] R. Krishna, A. J. Dreher, M. I. Urseanu, *Int. Commun. Heat Mass. Transf.* **2000**, *27*, 465-472.

[16] R. Krishna, M. I. Urseanu, A. J. Dreher, *Chem. Eng. Process.: Process Intensif.* **2000**, *39*, 371-378.

[17] R. Krishna, J. Ellenberger, C. Maretto, *Int. Commun. Heat Mass. Transf.* **1999**, *26*, 467-475.

[18] Y. T. Shah, B. G. Kelkar, S. P. Godbole, W.-D. Deckwer, *AIChE J.* **1982**, *28*, 353-379.

[19] S. Nedeltchev, S. B. Kumar, M. P. Dudukovic, *Can. J. Chem. Eng.* **2003**, *81*, 367-374.

[20] S. Nedeltchev, A. Shaikh, M. Al-Dahhan, *Chem. Eng. & Techn.* **2011**, *34*, 225-233.

[21] R. Kikuchi, T. Yano, A. Tsutsumi, K. Yoshida, M. Punchochar, J. Drahos, *Chem. Eng. Sci.* **1997**, *52*, 3741-3745.

[22] S. Nedeltchev, U. Hampel, M. Schubert, *Chem. Eng. Res. & Des.* **2016**, *115*, 303-309.

[23] W. Zhong, X. Wang, Q. Li, B. Jin, M. Zhang, R. Xiao, Y. Huang, *Can. J. Chem. Eng.* **2009**, *87*, 220-227.

[24] S. Nedeltchev, Y. Top, M. W. Hlawitschka, M. Schubert, H.-J. Bart, *Can. J. Chem. Eng.* **2020**, *98*, 1607-1621.

[25] S. Nedeltchev, S. Rabha, U. Hampel, M. Schubert, *Chem. Eng. & Techn.* **2015**, *38*, 1940-1946.

[26] H. Im, J. Park, J. W. Lee, *ACS Omega* **2019**, *4*, 1329-1343.

[27] J. Jia, M. Wang, Y. Faraj, *Measurement Science and Technology* **2014**, *26*, 015305.

[28] Q. Wang, J. Polansky, B. Karki, M. Wang, K. Wei, C. Qiu, A. Kenbar, D. Millington, *Journal of Hydrodynamics, Ser. B* **2016**, *28*, 1018-1021.

[29] F. Dickin, M. Wang, *Measurement Science and Technology* **1996**, *7*, 247.

[30] M. Wang, *Measurement Science and Technology* **2001**, *13*, 101.

[31] D. L. George, J. R. Torczynski, K. A. Shollenberger, T. J. O'Hern, S. L. Ceccio, *International Journal of Multiphase Flow* **2000**, *26*, 549-581.

[32] A. Ajbar, W. Al-Masry, E. Ali, *Chem. Eng. & Process.* **2009**, *48*, 101-110.

[33] T. Wang, J. Wang, Y. Jin, *Chem. Eng. Sci.* **2005**, 60, 6199-6209.

[34] I. G. Reilly, D. S. Scott, T. J. W. De Bruijn, D. MacIntyre, *Can. J. Chem. Eng.* **1994**, *72*, 3-12.

[35] C. Vial, R. Laine, S. Poncin, N. Midoux, G. Wild, *Chem. Eng. Sci.* **2001**, *56*, 1085-1093.

[36] C. L. Hyndmann, F. Larachi, C. Guy, *Chem. Eng. Sci.* **1997**, *52*, 63-77.

[37] H. Hikita, S. Asai, K. Tanigawa, K. Segawa, M. Kitao, *Chem. Eng. J.* **1980**, *20*, 59-67.

[38] M. Jamialahmadi, H. Műller-Steinhagen, *Chem. Eng. J.* **1992**, *50*, 47-56.

[39] E. M. Al-Oufi, C. D. Rielly, I. W. Cumming, *Chem. Eng. Sci.* **2011**, *66*, 5739-5748.

[40] G. Besagni, F. Inzoli, G. De Guido, L. A. Pellegrini, *Chem. Eng. Res. Des.* **2016**, *112*, 1-15.

[41] C. Leonard, J.-H. Ferrasse, O. Boutin, S. Lefevre, A. Viand, *Chem. Eng. Res. Des.* **2015**, *100*, 391-421.

Short text to attract readers

New hybrid index (NHI) has been introduced on the basis of the information entropy theory to identify accurately the main transition velocities in several bubble columns operated with water and

aqueous alcoholic solutions (ethanol and iso-propanol). The first transition velocity (end of homogeneous regime) is precisely identifiable based on a well-pronounced local NHI minimum. However, the onset of the heterogeneous regime is not so clearly distinguishable. The point at which the NHI profile levels off marks the second transition, i.e. the onset of liquid macrocirculation and bubble coalescence in the case of air-water system. It has been found in aqueous solutions of alcohols that a complete foaming regime is formed at high gas velocities. Both transition velocities depend on the type of gas-liquid system and gas sparger used.

Table and figure captions

Table 1. Overview of the various identification parameters in bubble columns.

Table 2. Physicochemical properties of ethanol and aqueous solutions of alcohols used.

Table 3. Summary of the identified main transition velocities and comparison with the predictions of the widely used semi-empirical correlations in the literature.

Figure 1. Experimental setup for the ERT measurements (left) and photography of the used cross-sparger (right).

Figure 2. FR boundaries identified by means of the NHI values extracted from: (a) ERT data in a BC (0.1 m in ID) operated with an air-deionized water system (L_0=1.0 m); (b) aerated height fluctuations in a BC (0.1 m in ID) operated with an air-deionized water system (L_0=1.0 m); (c) DP fluctuations in a BC (0.1 m in ID) operated with a nitrogen-tap water system (L_0=1.3 m).

Figure 3. Gas holdup profile recorded by an ERT facility in an air-water BC (0.1 m in ID) equipped with a cross-sparger 12 orifices × ∅ 1.0 mm).

Figure 4. FR boundaries identified by means of the NHI values extracted from: (a) DP fluctuations in a BC (0.1 m in ID) operated with a nitrogen-ethanol system (L_0=1.3 m); (b) GP fluctuations in a BC (0.1 m in ID) operated with air and an aqueous solution of ethanol (deionized water + 0.5 wt. % ethanol) (L_0=1.1 m).

Figure 5. FR boundaries identified by means of the NHI values in an aqueous solution of iso-propanol (deionized water + 0.5 wt. % iso-propanol) aerated in a BC (0.1 m in ID, L_0=1.1 m).